Excitonic absorption edge in alkali halides and the Urbach-Martienssen rule studied by three-photon difference-frequency generation

D. Fröhlich, P. Köhler, W. Nieswand, and T. Rappen
Institut für Physik, Universität Dortmund, 4600 Dortmund 50, Federal Republic of Germany

E. Mohler
Physikalisches Institut der Universität Frankfurt, 6000 Frankfurt am Main, Federal Republic of Germany
(Received 14 December 1990)

Three-photon difference-frequency generation (TP-DFG) is used to excite resonances on the lower exciton-polariton branch in alkali halides. The line shape of the resonances is investigated in KI and RbI for temperatures between 1.5 and 800 K. A drastic variation of the linewidth ranging from 0.2 to about 50 meV is observed as a function of temperature and polariton energy. The experimental results are interpreted in the framework of polariton response theory, which links the shape of the TP-DFG resonance to the complex dielectric function. From the measured positions and widths of the resonance peaks, accurate data on dispersion and absorption are obtained for the region of the exponential tail of the excitonic absorption edge. The method allows us to determine the parameters of the Urbach-Martienssen rule by measurements on large single crystals.

I. INTRODUCTION

The investigation of absorption bands of excitons and of the accompanying dispersion of the refractive index has a long tradition. There are different linear and nonlinear optical methods to study these phenomena in crystalline solids. For a review we refer to Hönerlage *et al.*[1] and Bassani and Andreani.[2] With conventional linear optical experiments like measurement of reflection, refraction, and absorption one essentially determines the frequency dependence of the optical constants and derives exciton energies from the observed resonances of these quantities. Because of high absorption in the resonance region, transmission measurements have to be done on very thin crystals or on evaporated layers. The experimental results might therefore be affected by strain and other perturbations. Although reflection data can be taken from bulk crystals, care is necessary to prepare good quality optical surfaces. If the Kramers-Kronig relations are applied to determine the optical constants the reflectivity measurements have to be done throughout a sufficiently extended spectral range. In spite of these difficulties, the optical data obtained by linear spectroscopic methods have been fundamental for our understanding of the electronic structure of the solid state.

Nonlinear optical spectroscopy opens up new possibilities to study elementary excitations in solids. Because of additional degrees of freedom in experiments where more than one photon is participating, new or more precise information can be gained which might not be accessible to one-photon experiments. In particular, nonlinear spectroscopy allows us to study directly the coupled states of excitons and photons called polaritons. Longitudinal excitons which are normally forbidden in one-photon spectroscopy can also be excited by nonlinear methods. Since the properties of excitons and polaritons are connected to each other within the dielectric theory, the information obtained by nonlinear methods is frequently equivalent to that resulting from linear methods. However, nonlinear spectroscopy allows us, in many cases, to circumvent some of the drawbacks of linear spectroscopy mentioned above.

Polariton resonances in alkali halides cannot be detected by two-photon techniques as it is possible in zinc blende or other crystals without an inversion center.[1] In order to exhibit a polariton structure the exciton in question has to be one-photon allowed. In crystals with inversion symmetry such an excitation cannot simultaneously be two-photon allowed if one considers dipole transitions only. One therefore has to resort to three-photon techniques. With the method of three-photon absorption (TPS) Beerwerth and Fröhlich[3] studied the polariton dispersion and the longitudinal exciton in KI and CsI. The measurements were extended to other alkali halides by Beerwerth *et al.*[4] Recently, Fröhlich *et al.*[5] introduced three-photon difference-frequency generation (TP-DFG) to excite resonances on the lower polariton branch in KI and RbI. At low temperatures these resonances show a spectacularly small linewidth of only about 0.2 meV which, e.g., allows us to study the splitting of the polariton branch in a magnetic field.[6]

In the experiments mentioned so far three-photon techniques were mainly used to investigate the structure of the polariton branches and to determine the real part of the dielectric function from the energetic positions and the wave-vector dependence of the resonances. The aim of the present contribution is to demonstrate that a complete set of optical constants can be obtained by a supplementary analysis of the TP-DFG linewidth which is connected to the imaginary part of the dielectric function. With this method, the frequency and temperature dependence of the absorption constant can be studied at the ex-

 ©1991 The American Physical Society

citonic absorption edge. The spectral shape and the temperature dependence of the absorption in this region are described by the Urbach-Martienssen rule[7,8] which has gained much interest due to its applicability to a large variety of compounds[9] and because of different competing models which have been suggested for its quantum-mechanical interpretation.[10–12] With the TP-DFG method it is possible to determine the parameters of the Urbach-Martienssen rule from absorption data measured in a rather unconventional way on large single crystals.

II. EXPERIMENTAL METHOD

The principle of TP-DFG spectroscopy is shown in Fig. 1 for a typical resonance on the lower exciton-polariton branch. Polaritons $(\hbar\omega,\mathbf{k})$ with energy $\hbar\omega$ and wave vector $\mathbf{k}$ are created by the absorption of two polaritons $(\hbar\omega_1,\mathbf{k}_1)$ and by stimulated emission of a third polariton $(\hbar\omega_3,\mathbf{k}_3)$. For this process the resonance conditions

$$\hbar\omega=2\hbar\omega_1-\hbar\omega_3 \quad \text{and} \quad \mathbf{k}=2\mathbf{k}_1-\mathbf{k}_3 \tag{1}$$

are valid. The beam of signal photons is detected at frequency ω in the direction of the total wave vector $\mathbf{k}$.

Details of the optical setup are given in a recent publication.[6] The absorbed polaritons $(\hbar\omega_1,\mathbf{k}_1)$ are excited by a tunable dye laser beam and the emission of polaritons $(\hbar\omega_3,\mathbf{k}_3)$ is induced by a fixed frequency Nd:YAG (neodymium-doped:yttrium-aluminum-garnet) laser beam or its harmonics and Raman shifted frequencies. The pump beams are colinear; note that one beam has to be directed antiparallel to the other.

The sample size is about $10\times10\times5$ mm^3 and the surfaces are prepared by cleaving. Measurements of temperature dependences are done by the use of a Janis helium cryostat (up to 100 K), a closed cycle helium refrigerator (up to 300 K), and a special furnace where the crystal is placed in a tube with quartz windows under argon atmosphere (up to 800 K). The temperature stability during a run (about 15 min) is better than ±0.1 K which is necessary because of the rather large temperature shift of the exciton resonance and the drastic temperature broadening of the absorption edge.

III. RESULTS

Figure 2 presents an overview of the accessible polariton resonance energies in KI as a function of wave vector and temperature. Different pump energies $\hbar\omega_3$ are necessary to scan the lower polariton branch in an energy and temperature range as large as possible. For a given pump energy the resonances at the lowest temperatures are marked with circles and with the symbols A–F. The adjoining lines show the trajectory of the resonance points through the fan of dispersion curves at higher temperatures. At the end of the trajectory the TP-DFG signals become too faint to be detected.

Figure 3 shows measured TP-DFG resonance lines in configuration F (pump energy $\hbar\omega_3=0.6497$ eV) at four different temperatures. The shape of the lines is fitted by Lorentzians. We observe a drastic broadening and a shift to lower energies with rising temperature. Figure 4 summarizes the data observed in KI for the peak energies $\hbar\omega_m$ of the resonances and for the full width at half maximum $\hbar\Delta\omega_{\mathrm{FHM}}$. Figure 5 contains the corresponding data for RbI. In each configuration the linewidth remains constant below a certain temperature. This limiting linewidth of about 0.2 meV is mainly determined by the resolution of the laser system.

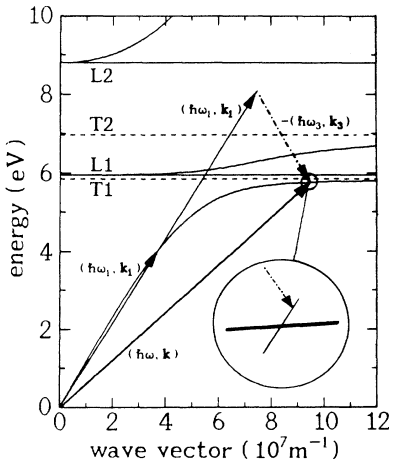

FIG. 1. Schematic presentation of TP-DFG on the lowest polariton branch. At resonance, the polariton dispersion curve (thick line in inset) is cut by the dispersion curve of the combined pump photons (thin line in inset). The horizontal lines $L1$, $L2$ (solid lines) and $T1$, $T2$ (dashed lines) mark the longitudinal and transverse energies, respectively, as given in Table I.

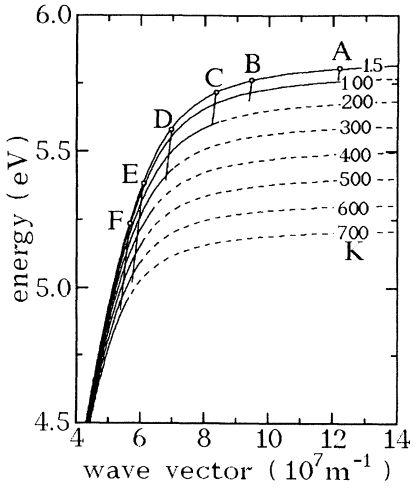

FIG. 2. Temperature dependence of polariton dispersion in KI. Circles and symbols A–F mark TP-DFG resonances at 1.5 K for different pump energies $\hbar\omega_3$ (A, 3.4943 eV; B, 2.3295 eV; C, 1.1845 eV; D, 1.1648 eV; E, 0.8034 eV; F, 0.6497 eV). The adjoining lines show the positions of the resonance points on the temperature shifted dispersion curves (dashed lines).

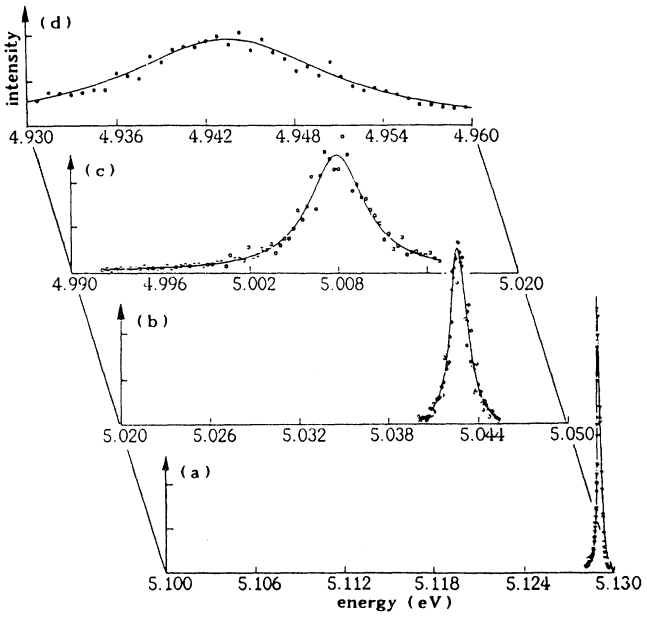

FIG. 3. TP-DFG resonances of KI at different temperatures in configuration F [(a) 300 K, (b) 465 K, (c) 525 K, (d) 625 K]. The resonance shape is approximated by Lorentzians to determine peak energies $\hbar\omega_m$ and halfwidths $\hbar\Delta\omega_{\mathrm{FHM}}$.

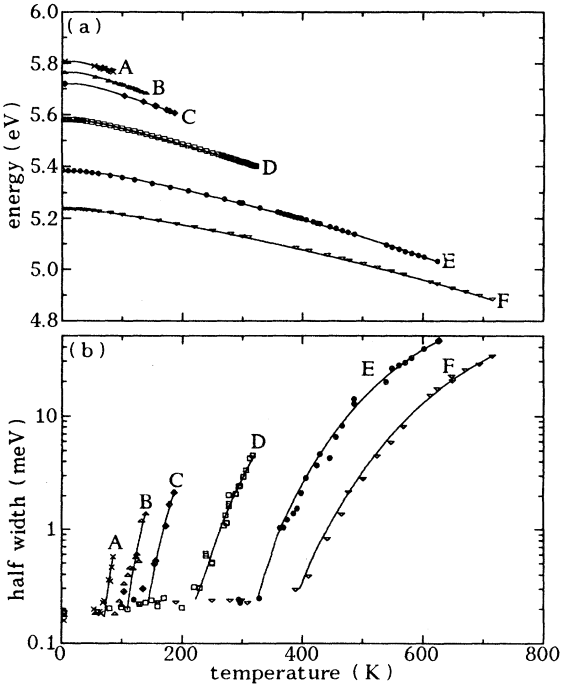

FIG. 4. Peak energies $\hbar\omega_m$ (a) and halfwidths $\hbar\Delta\omega_{\mathrm{FHM}}$ (b) of TP-DFG resonances in KI depending on temperature for different pump photon energies $\hbar\omega_3$ (configurations A–F). The curves are drawn as guides for the eye.

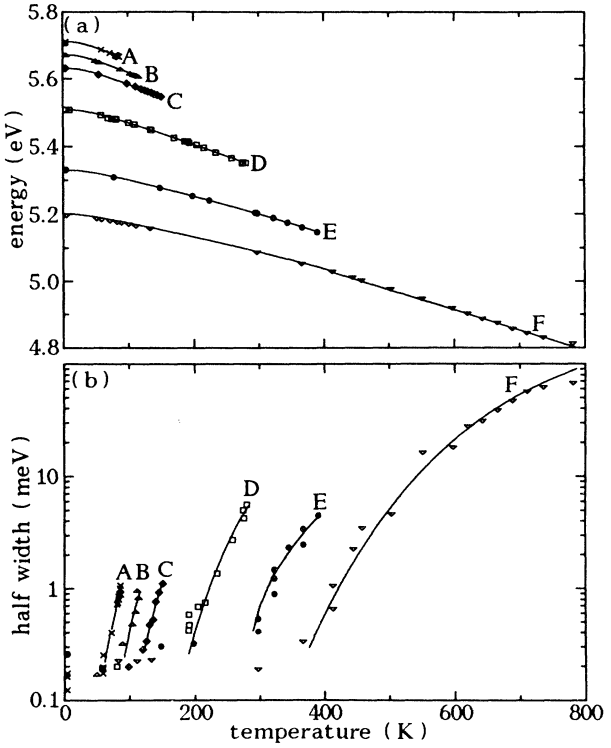

FIG. 5. Peak energies $\hbar\omega_m$ (a) and halfwidths $\hbar\Delta\omega_{\mathrm{FHM}}$ (b) of TP-DFG resonance in RbI depending on temperature for different pump photon energies $\hbar\omega_3$ (configurations A–F). The curves are drawn as guides for the eye.

IV. THEORY

In this section the line shape of the TP-DFG resonances is derived in the framework of polariton theory. We start with Maxwell's equations for dielectric media which lead to the polariton wave equation

$$\nabla^2\mathbf{E}-\nabla(\nabla\cdot\mathbf{E})-\frac{1}{c^2}\frac{\partial^2\mathbf{E}}{\partial t^2}=\frac{1}{c^2\epsilon_0}\frac{\partial^2\mathbf{P}}{\partial t^2}\ . \tag{2}$$

In Eq. (2), $\mathbf{E}$ is the electric field, c the velocity of light in vacuum, and ϵ_0 the permittivity of vacuum. The polarization can be written as $\mathbf{P}=\mathbf{P}_l+\mathbf{P}_{\mathrm{nl}}$ where $\mathbf{P}_l$ is the linear part due to the polariton response and $\mathbf{P}_{\mathrm{nl}}$ the nonlinear driving polarization with wave vector $2\mathbf{k}_1-\mathbf{k}_3$ and frequency $\omega=2\omega_1-\omega_3$ caused by the TP-DFG process. It is assumed that the depletion of the pump waves can be neglected. We have $\mathbf{P}_l=(\hat{\epsilon}-\hat{1})\epsilon_0\mathbf{E}$ where $\hat{\epsilon}$ is the dielectric tensor. If one regards transverse waves $\mathbf{E}$ with time dependence $e^{-i\omega t}$ imposed by the TP-DFG excitation and propagating along the z direction in an optically isotropic crystal, Eq. (2) simplifies to

$$\frac{\partial^2}{\partial z^2}E(z)+\frac{\omega^2}{c^2}\epsilon E(z)=-\frac{\omega^2}{c^2}\frac{P_0}{\epsilon_0}e^{i(2k_1+k_3)z}\ . \tag{3}$$

Here, ϵ is the scalar dielectric function and P_0 the component of $\mathbf{P}_{\mathrm{nl}}$ transverse to z. The electric field of magnitude $E(z)$ is also directed along this projection. Further,

the wave-vector configuration $\mathbf{k}_3 \| \mathbf{k}_1 \| \mathbf{z}$ is assumed. The general solution of the inhomogeneous differential equation Eq. (3) can be written as

$$E(z)=c_1 e^{ik_0\sqrt{\epsilon}z}+c_2 e^{-ik_0\sqrt{\epsilon}z}+a e^{ik_0\sqrt{\eta}z}, \tag{4}$$

where $k_0=\omega/c$ is the vacuum wave vector and $k_0\sqrt{\eta}=(2k_1+k_3)$ is the sum wave vector of the pump wave. The quantity $\sqrt{\eta}$ is introduced as an effective refractive index which is determined by the refractive indices of the pump waves [Eq. (12)]. The first two terms in Eq. (4) are free spatial oscillations solving the homogeneous equation and the third term corresponds to forced spatial oscillations induced by the inhomogeneous part. The amplitude of the forced wave is given by $a=RP_0/\epsilon_0$ where

$$R=\frac{1}{\eta-\epsilon} \tag{5}$$

is the polariton response function which describes the response of the transverse electric field to the nonlinear driving polarization.[13]

The constants of integration c_1 and c_2 have to be determined from the boundary conditions which link the polariton electric field inside the crystal to electric fields of frequency ω outside the crystal. As sketched in Fig. 6 there is a backward running field $E_b=be^{-ik_0z}$ and a forward running field $E_f=fe^{ik_0z}$ radiated from the crystal. The Maxwell boundary conditions at $z=0$ and L, where L is the length of the crystal, lead to four equations:

$$b=c_1+c_2+a, \tag{6a}$$

$$-b=c_1\sqrt{\epsilon}-c_2\sqrt{\epsilon}+a\sqrt{\eta}, \tag{6b}$$

$$fe^{i\Phi}=c_1 e^{i\sqrt{\epsilon}\Phi}+c_2 e^{-i\sqrt{\epsilon}\Phi}+a e^{i\sqrt{\eta}\Phi}, \tag{6c}$$

$$fe^{i\Phi}=c_1\sqrt{\epsilon}\,e^{i\sqrt{\epsilon}\Phi}-c_2\sqrt{\epsilon}\,e^{-i\sqrt{\epsilon}\Phi}+a\sqrt{\eta}\,e^{i\sqrt{\eta}\Phi}, \tag{6d}$$

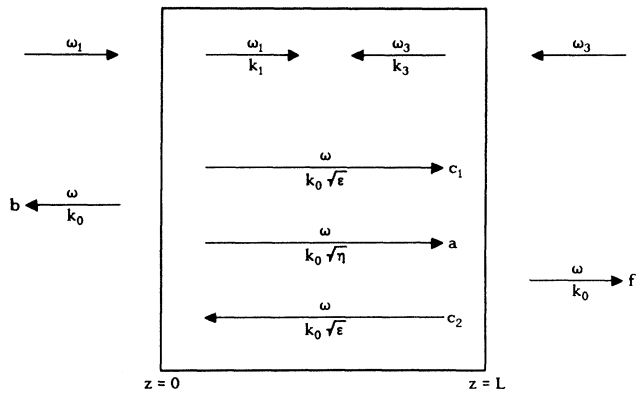

FIG. 6. Schematic presentation of waves involved in the TP-DFG process. Uppermost arrows mark pump waves, lower arrows indicate induced waves inside and outside the crystal. Frequencies and magnitude of relevant wave vectors are given above and below the arrows, respectively.

with $\Phi=k_0L$. Equations (6a)–(6d) are sufficient to derive c_1, c_2, b, and f as functions of a and the other parameters. The detailed expressions for these quantities will not be discussed here, since in the following we consider the case where the absorption length of the polariton wave is much smaller than the crystal length. This situation is met in most of the present experiments. Introducing the complex refractive index $\tilde{n}=n+i\kappa=\sqrt{\epsilon}$ and the absorption constant $\alpha=2k_0\kappa$ we have $\sqrt{\epsilon}\Phi=k_0nL+i\alpha L/2$. For the limit $\alpha \gg 1/L$ we obtain

$$c_1=-a(1+\sqrt{\eta})/(1+\sqrt{\epsilon}), \tag{7a}$$

$$c_2=0, \tag{7b}$$

$$b=a(\sqrt{\epsilon}-\sqrt{\eta})/(1+\sqrt{\epsilon}), \tag{7c}$$

$$f=a(\sqrt{\epsilon}+\sqrt{\eta})e^{i(\sqrt{\eta}-1)\Phi}/(1+\sqrt{\epsilon}). \tag{7d}$$

In deriving Equations (7a)–(7d) note that although c_2 goes to zero, the quantity $c_2e^{-i\sqrt{\epsilon}\Phi}$ remains finite.

Our experiment monitors the intensity of light of frequency ω radiated from the pumped crystal. Therefore we are interested in the intensities $I_b=\frac{1}{2}\epsilon_0 c|b|^2$ and $I_f=\frac{1}{2}\epsilon_0 c|f|^2$. It is assumed that the function η is a real quantity because the pump frequencies ω_1 and ω_3 are far away from the absorption region and we neglect depletion of the pump waves due to the nonlinear processes. We finally obtain

$$I_b=\frac{1}{2}\epsilon_0 c\frac{1}{|1+\sqrt{\epsilon}|^2|\sqrt{\eta}+\sqrt{\epsilon}|^2}\left|\frac{P_0}{\epsilon_0}\right|^2 \tag{8}$$

and

$$I_f=\frac{1}{2}\epsilon_0 c\frac{1}{|1+\sqrt{\epsilon}|^2|\sqrt{\eta}-\sqrt{\epsilon}|^2}\left|\frac{P_0}{\epsilon_0}\right|^2. \tag{9}$$

The signals I_b and I_f show marked structures as a function of ω which are caused by the ϵ- and η-dependent prefactors. The phenomenon of most interest in the present investigation is observed in the intensity I_f where a resonance is produced if $(\sqrt{\eta}-\sqrt{\epsilon})$ comes close to zero. This condition is fulfilled if $2k_1+k_3=\omega n/c$. It expresses the phase matching between the free running polariton wave and the nonlinear polarization. It is easily seen that the position of the resonance is mainly determined by the real part and the width of the resonance by the imaginary part of the complex refractive index $\tilde{n}=\sqrt{\epsilon}$.

V. DATA EVALUATION

The aim of the following section is to determine the complex dielectric function ϵ in the spectral range covered by the TP-DFG resonances. The measured peak energies and half-widths of the resonance lines are used to fit the parameters of appropriate phenomenological expressions for the real and imaginary part of ϵ. From these, other optical constants may be calculated.

Using Eq. (9) the observed TP-DFG signal can be expressed as

$$I_f=\frac{1}{2}\epsilon_0 c\left|\frac{\sqrt{\eta}+\sqrt{\epsilon}}{1+\sqrt{\epsilon}}\right|^2\frac{1}{|\eta-\epsilon|^2}\left|\frac{P_0}{\epsilon_0}\right|^2. \tag{10}$$

The spectral shape of the resonance is mainly determined by the second fraction which is an absolute square of the polariton response function R introduced in Eq. (5). In the following, we neglect the weak frequency dependences of the other factors near the polariton resonance and discuss only $|R|^2$. We have

$$|R|^2=\frac{1}{[\eta(\omega)-\epsilon_1(\omega)]^2+\epsilon_2^2(\omega)}, \tag{11}$$

where $\epsilon_1(\omega)$ is the real and $\epsilon_2(\omega)$ the imaginary part of ϵ. The real quantity $\eta(\omega)$ is given by

$$\eta(\omega)=\left\{\frac{\omega+\omega_3}{\omega}\left[\epsilon_1\left[\frac{\omega+\omega_3}{2}\right]\right]^{1/2}+\frac{\omega_3}{\omega}[\epsilon_1(\omega_3)]^{1/2}\right\}^2. \tag{12}$$

The function $\epsilon_1(\omega)$ is approximated by an undamped two-oscillator expression

$$\epsilon_1(\omega)=\epsilon_b\frac{\omega_{L1}^2-\omega^2}{\omega_{T1}^2-\omega^2}\frac{\omega_{L2}^2-\omega^2}{\omega_{T2}^2-\omega^2}, \tag{13}$$

where ω_{T1} and ω_{L1} are the frequencies of the lowest transverse and longitudinal excitons, respectively, and ϵ_b, ω_{T2}, and ω_{L2} describe background oscillators. The function $\epsilon_2(\omega)$ is connected with the absorption constant $\alpha(\omega)$ by the relation $\epsilon_2(\omega)=\alpha(\omega)n(\omega)c/\omega$. At the absorption edge, $\alpha(\omega)$ follows the Urbach-Martienssen rule,

$$\alpha(\omega)=\alpha_0\exp\left[\frac{\sigma}{k_BT}(\hbar\omega-E_n)\right], \tag{14}$$

where α_0, σ, and E_n are empirically determined material parameters, T is the temperature, and k_B is Boltzmann's constant. Although the assumption of an undamped $\epsilon_1(\omega)$ in the presence of absorption formally violates the Kramers-Kronig relations, the error introduced in $\epsilon_1(\omega)$ is negligible in the region of the absorption edge which is investigated by the TP-DFG experiment.

The shape of the TP-DFG resonance lines is analyzed in the following way. We define the frequency ω_0 where the phase-matching condition $\epsilon_1(\omega_0)=\eta(\omega_0)$ is fulfilled. Introducing the detuning $\Delta\omega=\omega-\omega_0$ we use the expansion $\epsilon_1(\omega)-\eta(\omega)=A\Delta\omega$ where $A=d/d\omega[\epsilon_1(\omega)-\eta(\omega)]_{\omega=\omega_0}$. In view of Eq. (14) we approximate $\epsilon_2(\omega)$ by $\epsilon_2(\omega)=\epsilon_2(\omega_0)\exp[\sigma\hbar\Delta\omega/k_BT]$. The response $|R|^2$ can then be written in reduced form as

$$|R|^2=\frac{C}{x^2+e^{BX}} \tag{15}$$

with $C=1/\epsilon_2^2(\omega_0)$, $B=2\hbar\sigma\epsilon_2(\omega_0)/(k_BTA)$, and $x=A\Delta\omega/\epsilon_2(\omega_0)$. For $B\ll1$ the resonance has the shape of a symmetrical Lorentzian centered at $x=0$. In this limit the frequency of the peak maximum is given by $\omega_m=\omega_0$ and the full width at half maximum is $\Delta\omega_{\mathrm{FHM}}=2\epsilon_2(\omega_0)/A$. For increasing B the peak maximum is shifted to lower energies and the full halfwidth is reduced. These corrections can be obtained numerically from Eq. (15) and are taken into account in the data evaluation. The shape of the peak also becomes asymmetrical, but details of these distortions are neglected.

The dielectric function is fitted by iteration. We use fixed values of ϵ_b, ω_{T2}, ω_{L2}, and $\omega_{L1}-\omega_{T1}$ as listed in Table I. These data were derived earlier by a careful analysis of the polariton branches known from three-photon spectra.[6] The parameter σ is given an approximate but fixed value. In the first step of the iteration ω_0 is determined from the measured ω_m assuming $B=0$. Then ω_{T1} is fitted to reproduce this ω_0. This allows us to calculate A and to obtain $\epsilon_2(\omega_0)$ from the measured $\Delta\omega_{\mathrm{FHM}}$. The procedure is repeated with $B\neq0$ calculated from A and $\epsilon_2(\omega_0)$. About ten further iterations are sufficient to determine "self-consistent" values of $\omega_{T1}(T)$ and $\epsilon_2(\omega_0,T)$. For ϵ_2 only those data are evaluated where $\Delta\omega_{\mathrm{FHM}}$ is sufficiently above the resolution limit. The calculations can then be redone with an improved value of σ obtained by an analysis of $\alpha(\omega,T)$ as described in detail later.

The upper curves in Figs. 7 and 8 show the temperature dependences of the exciton energies $\hbar\omega_{T1}$ for KI and RbI, respectively. The data are fitted by the function

$$\hbar\omega_{T1}(T)=\hbar\omega_{T1}(0)+D\left[1-\coth\left[\frac{\hbar\Omega}{2k_BT}\right]\right]. \tag{16}$$

An expression of this kind is often used to describe temperature variations of lattice properties which are expected to depend on the mean thermal energy of phonons (with effective frequency $\hbar\Omega$). The factor D takes into account both the self energy of the exciton and the influence of lattice dilatation. Table II shows the parameters resulting from the fit. The value of $\hbar\omega_{T1}(0)$ is taken from Ref. 6. Above about 100 K the temperature shift of ω_{T1} becomes linear. In this limit, the temperature coefficient $S=d/dT(\hbar\omega_{T1})$ of the shift is given by $S=-2k_BD/\hbar\Omega$. The values of S are also listed in Table II.

TABLE I. Parameters of the two-oscillator model used for evaluation of the TP-DFG data.

	ϵ_b	$\hbar\omega_{T2}$ (eV)	$\hbar\omega_{L2}$ (eV)	$\hbar\omega_{T1}$ (eV)	$\hbar\omega_{L1}-\hbar\omega_{T1}$ (eV)
KI	1.64	6.97	8.81	5.847	0.099
RbI	1.74	6.76	8.19	5.748	0.098

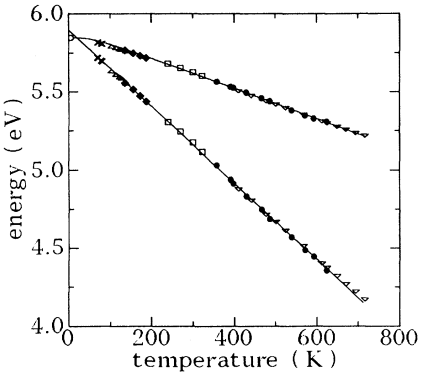

FIG. 7. Results of analysis of the TP-DFG resonances in KI. The upper curve shows the temperature dependence of the transverse exciton energy $\hbar\omega_{T1}$ fitted with expression Eq. (16). In the lower curve a specific combination of ω_0, T, and α is plotted vs T to give a straight line which allows us to determine the Urbach-Martienssen parameters. The open circle marks the transverse exciton energy at low temperatures as determined in Ref. 6.

The temperature coefficients found here are slightly larger than those observed in one-photon spectroscopy. Data from literature[8,14] referring to the shift of the absorption peak maximum are $S(\mathrm{KI})=8.34\times10^{-4}$ eV/K and $S(\mathrm{RbI})=7.69\times10^{-4}$ eV/K. Part of the deviations might be due to the fact that our dielectric model does not take into account a temperature dependence of the background oscillators. It should also be kept in mind that the peak maximum in one-photon absorption does not coincide with $\hbar\omega_{T1}$. The effective phonon frequencies $\hbar\Omega$ obtained from the fit are close to the optical phonon frequencies.

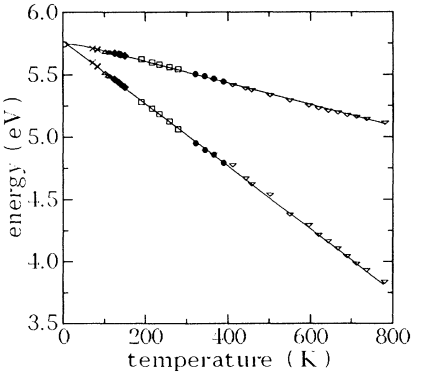

FIG. 8. Results of analysis of the TP-DFG resonances in RbI. The upper curve shows the temperature dependence of the transverse exciton energy $\hbar\omega_{T1}$ fitted with expression Eq. (16). In the lower curve a specific combination of ω_0, T, and α is plotted vs T to give a straight line which allows us to determine the Urbach-Martienssen parameters. The open circle marks the transverse exciton energy at low temperatures as determined in Ref. 6.

TABLE II. Parameters of temperature dependence of the transverse exciton energy $\hbar\omega_{T1}$ [see Eq. (16)] as derived from the TP-DFG data.

	$\hbar\omega_{T1}(0)$ (eV)	D (meV)	$\hbar\Omega$ (meV)	S (10^{-4} eV/K)
KI	5.847	74.1	12.9	9.86
RbI	5.748	39.8	7.8	8.77

We now turn to the imaginary part $\epsilon_2(\omega_0,T)$ and to the absorption function $\alpha(\omega_0,T)$ resulting from the evaluation of the TP-DFG resonances. One usually plots $\ln\alpha$ against $\hbar\omega_0$ for fixed T to determine the parameters α_0, σ, and E_n of the Urbach-Martienssen rule. One gets a bundle of straight lines intersecting in one point from which the parameters can be obtained graphically. This method is not favorable here because $\hbar\omega_0$ and T cannot be varied independently for a fixed pump energy. Instead, we proceed in a slightly modified way: Eq. (14) can be written in the form (note that $\omega=\omega_0$)

$$\hbar\omega_0-\frac{k_BT}{\sigma}\ln\alpha=E_n-\frac{k_BT}{\sigma}\ln\alpha_0\ . \tag{17}$$

One recognizes that the expression on the left-hand side of Eq. (17) should also give a straight line if plotted against T, provided that the experimental input data ω_0,α,T are combined with the correct σ. This criterium can be used to determine σ, E_n, and α_0 by a least-squares fit. The lower curves in Figs. 7 and 8 show that a very good fit is obtained. The parameters for KI and RbI are listed in Table III. To our knowledge the parameters of the Urbach-Martienssen rule for RbI are determined for the first time.

The parameters for KI determined by the TP-DFG analysis differ slightly from values known from the literature ($\sigma=0.82$, $E_n=5.89$ eV, $\alpha_0=5.9\times10^9$ cm^{-1}).[14]

It is surprising that σ derived here is smaller than the value obtained by one-photon absorption. One expects that the absorption edge measured in unperturbed bulk crystals should be steeper (i.e., σ should be larger) than in thin layers prepared for one-photon spectroscopy.

TABLE III. Parameters of the Urbach-Martienssen rule [see Eq. (14)] for the excitonic absorption edge as determined from the TP-DFG data.

	σ	E_n (eV)	α_0 (10^9 cm^{-1})
KI	0.79	5.898	5.03
RbI	0.70	5.775	6.26

VI. CONCLUSION

We have demonstrated that TP-DFG is a powerful method to study the lower exciton-polariton branch in alkali halides. Although TP-DFG by definition is a nonlinear optical method, the essential properties of the observed resonances can already be understood on the basis of linear polariton response theory. The analysis allows a quite accurate determination of the complex dielectric function in the region of the excitonic absorption edge. As central results, the temperature dependence of the transverse exciton energy and the parameters of the Urbach-Martienssen rule can be obtained from the TP-DFG data.

The TP-DFG method allows us to cover absorption values up to approximately 2×10^4 cm^{-1}. The investigation by one-photon techniques would already require the preparation of very thin samples supported by substrates of a nonabsorbing and therefore different material. The TP-DFG signal also originates from a very thin layer near the surface determined by the absorption length $l=1/\alpha$, but here the crystal serves as its own ideally matched substrate. This is possible because the surface region can be excited through the bulk which is transparent for the pump waves.

[1]B. Hönerlage, R. Lévy, J. B. Grun, C. Klingshirn, and K. Bohnert, Phys. Rep. **124**, 161 (1985).
[2]F. Bassani and L. C. Andreani, in *Excited State Spectroscopy in Solids*, Proceedings of the International School of Physics "Enrico Fermi," edited by U. W. Grassano and N. Terzi (North-Holland, New York, 1987).
[3]F. Beerwerth and D. Fröhlich, Phys. Rev. Lett. **55**, 2603 (1985).
[4]F. Beerwerth, D. Fröhlich, P. Köhler, V. Leinweber, and A. Voss, Phys. Rev. B **38**, 4250 (1988).
[5]D. Fröhlich, St. Kirchhoff, P. Köhler, and W. Nieswand, Phys. Rev. B **40**, 1976 (1989).
[6]D. Fröhlich, St. Kirchhoff, P. Köhler, and W. Nieswand, Phys. Status Solidi B **158**, 267 (1980).
[7]F. Urbach, Phys. Rev. **92**, 1324 (1953).
[8]W. Martienssen, J. Phys. Chem. Sol. **2**, 257 (1957).
[9]M. V. Kurik, Phys. Status Solidi A **8**, 9 (1971).
[10]H. Sumi and Y. Toyozawa, J. Phys. Soc. Jpn. **31**, 342 (1971).
[11]J. D. Dow and D. Redfield, Phys. Rev. B **5**, 594 (1972).
[12]J. G. Liebler, S. Schmitt-Rink, and H. Haug, J. Lumin. **34**, 1 (1985); J. G. Liebler and H. Haug, Europhys. Lett. **14**, 71 (1991).
[13]D. Fröhlich, P. Köhler, W. Nieswand, T. Rappen, and E. Mohler, J. Lumin. **45**, 229 (1990).
[14]U. Haupt, Z. Phys. **157**, 232 (1959).